

Search for Highly-Ionizing Particles in pp Collisions During LHC Run-2 Using the Full MoEDAL Detector

B. Acharya,^{1,*} J. Alexandre,¹ P. Benes,² B. Bergmann,² S. Bertolucci,³ A. Bevan,⁴ R. Brancaccio,⁵ H. Branzas,⁶ P. Burian,² M. Campbell,⁷ S. Cecchini,³ Y. M. Cho,⁸ M. de Montigny,⁹ A. De Roeck,⁷ J. R. Ellis,^{1,10} M. Fairbairn,¹ D. Felea,⁶ M. Frank,¹¹ J. Hays,⁴ A. M. Hirt,¹² D. L.-J. Ho,¹³ P. Q. Hung,¹⁴ J. Janecek,² M. Kalliokoski,¹⁵ D. H. Lacarrère,⁷ C. Leroy,¹⁶ G. Levi,⁵ A. Margiotta,⁵ R. Maselek,^{17,18} A. Maulik,^{3,9} N. Mauri,⁵ N. E. Mavromatos,^{1,†} M. Mieskolainen,¹⁹ L. Millward,⁴ V. A. Mitsou,^{20,†} A. Mukhopadhyay,⁹ E. Musumeci,²⁰ I. Ostrovskiy,²¹ P.-P. Ouimet,²² J. Papavassiliou,²⁰ L. Patrizii,^{3,‡} G. E. Pāvāļš,⁶ J. L. Pinfold,^{9,§} L. A. Popa,⁶ V. Popa,⁶ M. Pozzato,³ S. Pospisil,² A. Rajantie,¹³ R. Ruiz de Austri,²⁰ Z. Sahnoun,⁵ M. Sakellariadou,¹ K. Sakurai,¹⁸ S. Sarkar,¹ G. Semenoff,²³ A. Shaa,⁹ G. Sirri,³ K. Sliwa,²⁴ R. Soluk,⁹ M. Spurio,⁵ M. Staelens,²⁰ M. Suk,² M. Tenti,³ V. Togo,³ J. A. Tuszyński,⁹ A. Upreti,²¹ V. Vento,²⁰ and O. Vives²⁰

(THE MoEDAL COLLABORATION)

¹*Theoretical Particle Physics & Cosmology Group, Physics Dept., King's College London, UK*

²*IEAP, Czech Technical University in Prague, Czech Republic*

³*INFN, Section of Bologna, Bologna, Italy*

⁴*School of Physics and Astronomy, Queen Mary University of London, UK*

⁵*INFN, Section of Bologna & Department of Physics & Astronomy, University of Bologna, Italy*

⁶*Institute of Space Science, Bucharest - Măgurele, Romania*

⁷*Experimental Physics Department, CERN, Geneva, Switzerland*

⁸*Center for Quantum Spacetime, Sogang University, Seoul, Korea*

⁹*Physics Department, University of Alberta, Edmonton, Alberta, Canada*

¹⁰*Theoretical Physics Department, CERN, Geneva, Switzerland*

¹¹*Department of Physics, Concordia University, Montréal, Québec, Canada*

¹²*Department of Earth Sciences, Swiss Federal Institute of Technology, Zurich, Switzerland*

¹³*Department of Physics, Imperial College London, UK*

¹⁴*Department of Physics, University of Virginia, Charlottesville, Virginia, USA*

¹⁵*Helsinki Institute of Physics, University of Helsinki, Helsinki, Finland*

¹⁶*Département de Physique, Université de Montréal, Québec, Canada*

¹⁷*Laboratoire de Physique Subatomique et de Cosmologie,*

Université Grenoble-Alpes CNRS/IN2p3, Grenoble, France

¹⁸*Institute of Theoretical Physics, University of Warsaw, Warsaw, Poland*

¹⁹*Physics Department, University of Helsinki, Helsinki, Finland*

²⁰*IFIC, CSIC – Universitat de València, Valencia, Spain*

²¹*Department of Physics and Astronomy, University of Alabama, Tuscaloosa, Alabama, USA*

²²*Physics Department, University of Regina, Regina, Saskatchewan, Canada*

²³*Department of Physics, University of British Columbia, Vancouver, British Columbia, Canada*

²⁴*Department of Physics and Astronomy, Tufts University, Medford, Massachusetts, USA*

This search for Magnetic Monopoles (MMs) and High Electric Charge Objects (HECOs) with spins 0, 1/2 and 1, uses for the first time the full MoEDAL detector, exposed to 6.6 fb^{-1} proton-proton collisions at 13 TeV. The results are interpreted in terms of Drell-Yan and photon-fusion pair production. Mass limits on direct production of MMs of up to 10 Dirac magnetic charges and HECO with electric charge in the range $5e$ to $350e$, were achieved. The charge limits placed on MM and HECO production are currently the strongest in the world. MoEDAL is the only LHC experiment capable of being directly calibrated for highly-ionizing particles using heavy ions and with a detector system dedicated to definitively measuring magnetic charge.

The detection of a massive, stable or pseudo-stable, Highly-Ionizing Particle (HIP) with a significantly large electric charge $|q| \gg e$ (where e is the elementary charge) and/or a magnetic charge g_D , would provide compelling evidence for physics beyond the Standard Model. Many hypothetical particles capable of producing HIP signatures have been proposed, including Magnetic Monopoles (MMs) [1–12] and dyons [13]; Q-balls [14, 15]; micro black-hole remnants [16]; doubly charged massive particles [17]; scalars in neutrino-mass models [18]; and aggregates of ud - [19] or s -quark matter [20].

HIPs have been sought in matter [21], cosmic rays [21,

22] and in accelerator-based experiments [9, 12, 23], with recent searches conducted at the LHC [24–40].

According to the Dirac Quantization Condition [1], magnetic charge would be quantized in units of $g_D = e/2\alpha \approx 68.5e$, where α is the fine structure constant. Due to the exceptionally strong coupling between a MM and the photon, perturbative calculations cannot reliably predict cross-sections associated with MM production. The diagrams involved need to undergo appropriate resummation in order to account for potential non-perturbative quantum corrections [41, 42]. Such techniques have been investigated, especially for High Electric Charge

Objects (HECOs) [44]. For simplicity and ease of comparison with other search results, here we use leading-order Feynman diagrams for cross-section estimates.

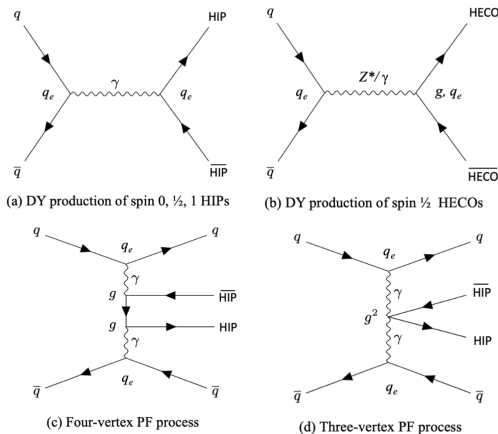


FIG. 1. Tree-level Feynman diagrams for the following: (a) DY production of HIP–anti-HIP pairs; (b) spin-1/2 HECO DY production; and, (c,d) PF production of HIP–anti-HIP pairs.

The Drell–Yan (DY) pair production mechanism provides a basic model for HIP creation. HIP pair production of spin-0, spin-1/2 and spin-1 are computed using the Feynman diagrams shown at the top of Fig. 1. Spin-1/2 HECO DY production can take place via virtual photon (γ) or γ/Z^0 exchange [45]. For DY production of spin-1/2 MMs, the coupling of the Z boson to magnetic charge is conventionally assumed to be absent. In some MM models, this can be proven explicitly [7, 46].

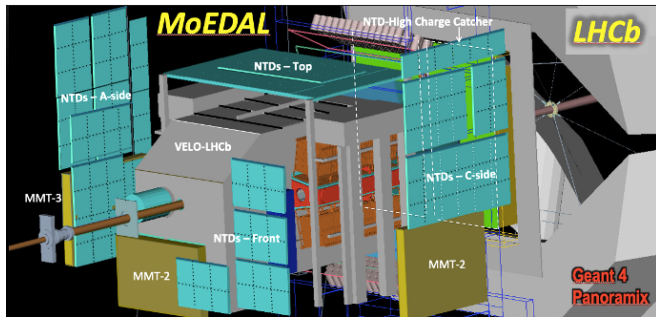


FIG. 2. A GEANT4 Panoramix view of the full MoEDAL detector deployed at IP8 during LHC’s Run-2.

Additionally, MoEDAL has pioneered the search for HIPs at the LHC using photon fusion (PF) [33, 47–49] described by the two Feynman diagrams shown at the bottom of Fig. 1. For the mass range considered here, PF production of HIPs has a considerable cross-sectional advantage compared to DY production [47]. Consequently, PF dominates when setting mass bounds. This picture is maintained even after resummation [41, 42, 44].

The physics processes considered here were generated using MADGRAPH5 [50] utilizing the Universal Feyn-Rules Output presented in Ref. [47]. The parton distribution functions (PDFs) NNPDF23 [51] and LUXqed [52] were used for the DY and PF production processes, respectively. The LUXqed PDF was created in a model-independent way utilizing ep scattering data.

In this search we used, for the first time, the full Run-2 MoEDAL detector shown in Fig. 2. MoEDAL’s detector technology differs radically from the general-purpose LHC experiments, ATLAS and CMS. The MoEDAL detector, positioned around LHCb’s Vertex LOcator detector (VELO) at IP8, employs two unconventional passive detection methodologies dedicated to HIP detection. The first is a system of plastic Nuclear Track Detectors (NTDs) — including the High-Charge Catcher (HCC) — designed to register HIP ionization trails. The second detector system, the Magnetic Monopole Trapper (MMT), is designed to capture HIPs that stop within its sensitive volume, allowing for further study at the ETH Zurich SQUID magnetometer facility.

Both NTD and MMT detector systems require neither readout electronics nor a trigger since no Standard Model (SM) particles can produce the distinctive signatures of HIPs traversing the MoEDAL detector. Thus, only a few HIP messengers of new physics observed in MoEDAL data are needed to herald a discovery. Below we give a brief description of the MoEDAL detector. A more detailed description of the detectors and their calibration and analysis is given in the supplemental material [53].

The NTD detector system is positioned around LHCb’s VELO detector, as presented in Fig. 2. It consists of an array of standard NTD stacks and the HCC, both of which are comprised of Makrofol NTD plastic. The HCC array is designed to extend the search for HIPs to the highest charge possible. This is achieved by situating the HCC between LHCb’s RICH1 detector and the first LHCb downstream tracking detector, TT1, minimizing the material in which the very highest ionizing particles may be absorbed. After exposure in the LHC’s IP8 region, the MoEDAL NTD stacks are sent to INFN Bologna for etching and scanning.

The pertinent quantity for MoEDAL’s plastic NTDs is the Restricted Energy Loss (REL) [54]. Heavy ion beams are used to determine the NTD response over a wide range of energy loss, as explained in Ref. [55]. The NTD response is calibrated directly using heavy-ion beams at the NASA Space Radiation Facility (NSRL) at the Brookhaven National Laboratory in the US and at the CERN SPS. The REL corresponding to the threshold of the Makrofol NTDs utilized is $\sim 2700 \text{ MeV g}^{-1} \text{ cm}^2$.

A study of the HIP detection efficiency of NTDs in the presence of beam backgrounds was performed by using NTD calibration stacks exposed to a relativistic lead-ion beam. The stacks were comprised of Makrofol NTD foils, exposed to beam backgrounds as part on MoEDAL’s

NTD array at LHC’s Run-2 during 2018, interleaved with previously *unexposed* Makrofol NTD sheets using plastic from the same production batch utilized in calibration and standard data taking. The NTDs sheets comprising the calibration stacks were then etched and scanned using the same techniques and procedures employed to examine all MoEDAL NTD stacks. As the relativistic lead-ion calibration beam particles penetrate the whole stack, the signal etch-pits seen in the LHC unexposed sheets can serve as a map of the passage of the heavy-ions. The identification efficiency of etch-pits in the LHC-unexposed sheets is measured to be effectively 100% by making independent comparison scans of the other LHC-unexposed sheets in the stack which have the identical etch-pit number and pattern.

During Run-2 the surface area of standard NTD stacks facing IP8 was 10.7 m². The corresponding area of HCC foils was 3.24 m². To avoid excessive damage from beam-induced backgrounds the standard stacks were replaced three times. The HCC foils were replaced more frequently, 7 times in all, as they were deployed nearer the beam line.

A pair of collinear incident and exiting etch-pits, found in the first layer of a 6-layer NTD stack, that are consistent with pointing to the IP, is defined as a “candidate”. The discovery of such a candidate would trigger the analysis of all 5 downstream foils comprising an NTD stack. A HIP “candidate track” requires collinear etch-pits pairs that point to the collision point in all six NTD sheets in the stack. No “candidate” or “candidate track” was found.

The MMT detector comprises 2400 aluminium bars with a mass of 800 kg deployed in three arrays transverse to and just forward of IP8. Aluminium was chosen as the trapping material because the aluminium nucleus has an anomalously large magnetic moment which engenders a monopole–nucleus binding energy of 0.5–2.5 MeV [57], which is consonant with the shell-model splittings. A MM will stop in the MMT if its speed falls below $\beta \leq 10^{-3}$. It will then bind to the nucleus due to the interaction between the MM and the nuclear magnetic moment [56–60]. MMs bound in such a way would be trapped indefinitely [56, 57].

After the MMT’s aluminium volumes were exposed for roughly a year they were sent to the ETH Zurich Laboratory for Natural Magnetism. They were passed through a SQUID magnetometer to check for trapped magnetic charges. The SQUID magnetometer calibration was performed using a known magnetic dipole sample and checked using a simulated MM comprised of long thin solenoids providing the same response as a MM with a known magnetic charge.

The acceptance of the MoEDAL detector at Run-2 is defined to be the fraction of events in which at least one HIP of the produced pair was detected in MoEDAL in either the NTD detector or the MMT detector, giv-

ing two sets of acceptance curves, one for each production mechanism considered. The acceptance for HECOs and MMs depends on an interplay between the positions of MoEDAL detector modules; energy loss in the detectors; the mass and charge of the particles; and the spin-dependent kinematics of the interaction products. For HECOs, MoEDAL’s NTD system provides the only means of detection. The spin-dependent acceptance for different spins are mostly due to the degree of coincidence of the azimuthal (ϕ) and polar (θ) distributions of the produced HIPs with that of the detector elements. Example acceptance curves are provided in the supplemental material [53]. The Run-2 geometric acceptance of MoEDAL’s NTD and MMT detectors for MMs partly overlap. Thus, care must be taken not to double-count signals when calculating the acceptance of the overall detector. Only the NTDs can be utilized for the HECO analysis since we cannot register HECOs trapped in the MMT detectors.

This analysis is dominated by systematic errors due to insufficient knowledge of the exact amount of material arising from the VELO detector, between the interaction point and the MoEDAL detector modules. The elements of the VELO detector within LHCb’s physics acceptance are naturally simulated with great precision in the LHCb geometry. However, the VELO elements outside of the LHCb’s physics acceptance were not sufficiently detailed to allow us to provide a precise estimate of the material budget. Estimates indicate the intervening material lying between the VELO detector the MoEDAL detector elements is between 0.1 and 8.0 radiation lengths (X_0) in thickness and on average, around $1.4X_0$ [62] in thickness. Two geometries provide upper and lower estimates of the uncertain amount of material described in the map. They are conservative estimates of uncertainties about material thicknesses and density, and they compare to the best assessment that is compatible both with direct measurements and existing drawings. The resulting relative uncertainty for singly charged MMs ($|g| = g_D$) is in the order of 10% [30]. The uncertainty increases with electric and magnetic charges. For doubly charged MMs ($|g| = 2g_D$) the uncertainty is around 10–20% for masses around 1 TeV.

Another source of systematic error is due to a conservative estimate of approximately 1 cm uncertainty in the trapping detector location. Simulations indicate this error is in the range 1–17% [30]. Additionally, a systematic error arises from the energy-loss uncertainty as a function of β , resulting in a 1–10% relative uncertainty in the acceptance [30]. Lastly, the error on the reduced etch rate, p , [53] leads to an error in the threshold value for the detection of plastic and an error in the variation of efficiency with angle. All the sources of (uncorrelated) systematic uncertainties on the overall efficiency of detection mentioned above were added in quadrature and included in the final limit calculation.

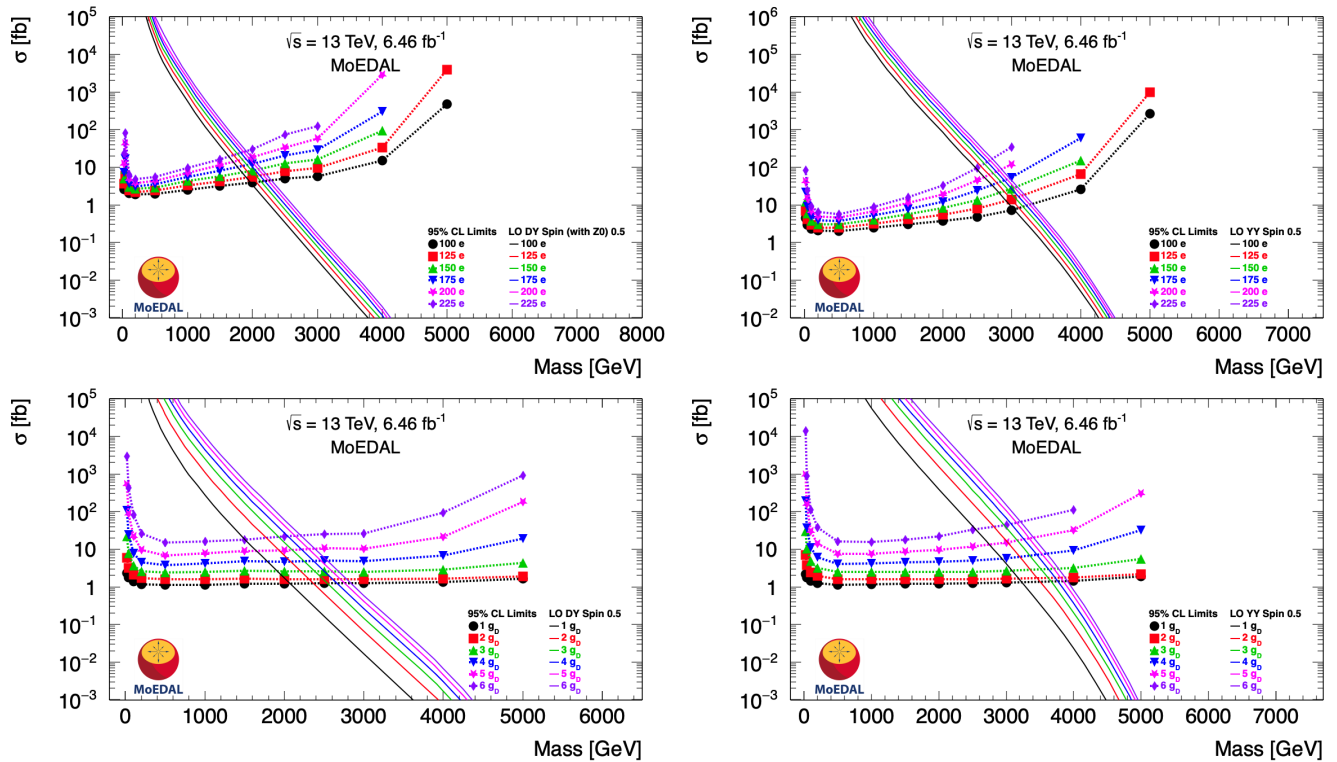


FIG. 3. 95% C.L. upper limits to the cross-section for the following production mechanisms: (Top Left) a DY model with virtual γ/Z^0 exchange for spin- $1/2$ production of HECOs with charge in the range $100e$ – $225e$; (Top Right) PF production of HECOs with charge q in the range $100e$ – $225e$; (Bottom Left) a DY model with virtual photon spin- $1/2$ production of MMs with magnetic charge in the range $1g_D$ – $6g_D$; and (Bottom Right) PF production of MMs with magnetic charge in the range $1g_D$ – $6g_D$. The solid lines denote the cross-section predictions for each case considered.

TABLE I. 95% CL mass limits for the magnetic monopole search.

Spin	Process	Magnetic charge (g_D)									
		1	2	3	4	5	6	7	8	9	10
0	DY	1450	1660	1730	1680	1590	1510	1380	1210	980	790
$1/2$	DY	2070	2300	2370	2360	2300	2200	2030	1810	1470	1040
1	DY	2180	2410	2510	2520	2460	2370	2240	2090	1870	1550
0	$\gamma\gamma$	2980	3210	3250	3200	3100	2950	2750	2500	–	–
$1/2$	$\gamma\gamma$	3210	3430	3490	3430	3320	3200	3020	2700	2510	–
1	$\gamma\gamma$	3620	3850	3890	3820	3710	3570	3400	3180	2790	–

No MM or HECO candidates were found after exposure of the MoEDAL detector to 6.46 fb^{-1} of pp collisions at a center-of-mass energy of 13 TeV during LHC's Run-2. Consequently, MoEDAL placed 95% confidence level (CL) lower mass limits on spin-1, spin- $1/2$ and spin-0 MM and HECO production. A complete set of limit curves for all HIP charge and mass points considered is included in the supplemental material [53].

Examples of the limit curves obtained for spin- $1/2$ HECOs produced via γ/Z^0 exchange and photon-fusion, with charges ranging from $100e$ – $225e$, are given in Fig. 3 (top left) and (top right), respectively. In the MM case, the example limit curves for MMs produced via DY and

photon-fusion with charge from $1g_D$ to $6g_D$ are shown in Fig. 3 (bottom left) and (bottom right), respectively.

The results of this MoEDAL search for MMs at the LHC reached a sensitivity to DY production cross-section in the range of approximately 1 fb to 5 pb. The mass limits as high as ~ 2.5 TeV were placed on magnetic charges up to $10g_D$. The corresponding 95% CL mass limits were placed on MMs produced via photon-fusion for: i) cross-section in the range of approximately 1 fb to 5 pb; ii) magnetic charge reaching up to $9g_D$; and iii) MM mass as high as ~ 3.4 TeV. MoEDAL's lower mass limits are summarized in Table I. A sample of the curves obtained for MMs produced by DY and photon-fusion are given in

TABLE II. 95% CL mass limits for the HECO search.

Spin	Process/ exchange	Electric charge (e)																	
		5	10	15	20	25	50	75	100	125	150	175	200	225	250	275	300	325	350
		95% CL mass limits (GeV)																	
0	DY γ	–	80	220	400	580	1300	1390	1420	1430	1430	1410	1390	1370	1340	1290	1210	1070	900
$1/2$	DY γ	–	290	620	920	1190	1850	1940	1980	2000	2000	1980	1940	1900	1830	1740	1610	1380	–
$1/2$	DY γ/Z^*	–	320	620	930	1170	1840	1930	1970	1990	1980	1970	1940	1900	1840	1740	1620	–	–
1	DY γ	–	330	640	960	1240	2020	2120	2170	2180	2180	2170	2140	2100	2060	1980	1850	1620	–
0	$\gamma\gamma$	440	910	1450	1880	2180	2710	2760	2770	2750	2710	2650	2590	2510	2390	2210	2020	–	–
$1/2$	$\gamma\gamma$	–	1110	1750	2180	2480	2980	3030	3030	2990	2940	2880	2810	2710	2580	2430	2220	–	–
1	$\gamma\gamma$	–	1600	2320	2730	3010	3360	3390	3380	3340	3300	3240	3160	3100	2980	2630	–	–	–

Fig. 3 (bottom left) and (bottom right), respectively.

Interpreting our results as a search for HECOs, we placed 95% CL lower mass limits on the following: i) HECO production via the DY mechanism for HECOs of spin-0, $1/2$ and 1; ii) cross-sections from around 1 fb to 10 pb; iii) electric charges in the range $10e \leq |q| \leq 350e$; and iv) mass limits ranging up to 2.2 TeV. For spin- $1/2$ HECOS, we also considered DY production via γ/Z^0 exchange. In this case, 95% CL mass limits were placed on HECO production with a cross-section in the range 1 fb to 2 pb; electric charges from $10e$ to $300e$; and mass limits as high as 2.0 TeV. In the case of HECOs produced via photon-fusion, 95% CL lower mass limits were placed on HECOs, with the following properties: spin- $1/2$, 0 and 1; cross-section in the range 1 fb to 4 pb; electric charges in the range $5e$ to $350e$. The corresponding mass limits, that range up to 3.4 TeV, are tabulated in Table II.

At the LHC, ATLAS is the only other experiment to have published searches for MMs and HECOs [35] based on DY production of MMs or HECOs and, much more recently, on PF and DY production [40].

MoEDAL's direct limits on the MM and HECO charge are by far the strongest published to date. Importantly, MoEDAL is the sole collider experiment to utilize dedicated detectors able to measure definitively the magnetic charge of the MM and also to be able to calibrate experimentally its detectors for HIPs directly using heavy-ions.

We thank CERN for the LHC's successful Run-2 operation, as well as the support staff from our institutions, without whom MoEDAL could not be operated. We acknowledge the invaluable assistance of particular members of the LHCb Collaboration: G. Wilkinson, R. Lindner, E. Thomas and G. Corti. In addition, we would like to recognize the valuable input from W.-Y. Song and W. Taylor of York University on HECO production processes. Computing support was provided by the GridPP Collaboration, in particular by the Queen Mary University of London and Liverpool grid sites. This work was supported by the UK Science and Technology Facilities Council, via the grants ST/L000326/1, ST/L00044X/1, ST/N00101X/1, ST/T000759/1 and ST/X000753/1; by the Generalitat Valenciana via the projects PROMETEO/2019/087,

CIPROM/2021/073 and CIAPOS/2021/88; by Spanish MICIN / AEI / FEDER, EU via the grant PID2021-122134NB-C21; by Spanish MUNI via the mobility grant PRX22/00633; by CSIC via the mobility grant IMOVE23097; by the Physics Department of King's College London; by NSERC via a project grant; by the V-P Research of the University of Alberta (UofA); by the Provost of the UofA); by UEFISCDI (Romania); by the INFN (Italy); by a National Science Foundation grant (US) to the University of Alabama MoEDAL group; and, by the National Science Centre, Poland, under research grant 2017/26/E/ST2/00135 and the Grieg grant 2019/34/H/ST2/0070.

* Also at Int. Centre for Theoretical Physics, Trieste, Italy

† Also at Department of Physics, School of Applied Mathematical and Physical Sciences, National Technical University of Athens, Athens, Greece

‡ Corresponding author: Laura.Patrizii@bo.infn.it

§ Corresponding author: jpinfold@ualberta.ca

- [1] P. A. M. Dirac, Quantised Singularities in the Electromagnetic Field, Proc. Roy. Soc.A 133, 60 (1931).
- [2] G. 't Hooft, Magnetic Monopoles in Unified Gauge Theories, Nucl. Phys. B79, 276 (1974).
- [3] A. M. Polyakov, Particle Spectrum in the Quantum Field Theory, JETP Lett.20, 194 (1974)
- [4] Y.M. Cho and D. Maison, Phys. Lett.B391, 360 (1997).
- [5] W.S. Bae and Y.M. Cho, J.Korean Phys.Soc, 791 (2005).
- [6] Y. M. Cho, K. Kim and J. H. Yoon, Eur. Phys. J. C75, no. 2, 67 (2015).
- [7] P. Q. Hung, Topologically stable, finite energy electroweak-scale monopoles, Nucl. Phys. B962, 115278 (2021).
- [8] J. Ellis, N. E. Mavromatos, T. You, The Price of an Electroweak Monopole, Phys. Lett. B756, 20-35 (2016).
- [9] Stable Massive Particles at Colliders, Phys. Rept. 438 (2007).
- [10] S. Balestra, G. Giacomelli, M. Giorgini, L. Patrizii, V. Popa, Z. Sahnoun and V. Togo, Magnetic Monopole Bibliography-II, May 2011. 32 pp. e-Print: arXiv:1105.5587 [hep-ex].
- [11] L. Patrizii and M. Spurio, Status of Searches for Magnetic Monopoles, Annu. Rev. Nucl. Part. Sci. 65, 279 (2015).
- [12] N. E. Mavromatos and V. A. Mitsou, Magnetic monopoles revisited: Models and searches at colliders

- and in the Cosmos, *Int. J. Mod. Phys. A* **35**, no.23, 2030012 (2020).
- [13] J. Schwinger, A Magnetic Model of Matter. *Science*. 165, 757-761 (1959).
- [14] S. Coleman, Q-balls, *Nucl. Phys. B* **262**, 263 (1985).
- [15] A. Kusenko and M. E. Shaposhnikov, Supersymmetric Q-balls as dark matter, *Phys. Lett. B* **418**(1998) 46.
- [16] B. Koch, M. Bleicher, and H. Stöcker, Black holes at LHC? *J. Phys. G* **34** S535 (2007).
- [17] B. Acharya et al., MoEDAL Collaboration, Physics Programme Of The MoEDAL Experiment At The LHC, *Int. J. Mod. Phys. A* **29**, 1430050 (2014).
- [18] M. Hirsch, R. Maselek and K. Sakurai, Detecting long-lived multi-charged particles in neutrino mass models with MoEDAL *Eur. Phys. J. C* **81** (2021) 8, 697; e-Print: 2103.05644 [hep-ph].
- [19] B. Holdom, J. Ren, and C. Zhang, Quark Matter May Not Be Strange, *Phys. Rev. Lett.* **120**, 222001
- [20] E. Farhi and R. Jaffe, Strange matter, *Phys. Rev. D* **30**, 2379 (1984).
- [21] S. Burdin et al., Non-collider searches for stable massive particles, *Phys. Rept.* **582**, 1 (2015).
- [22] L. Patrizzii, Z. Sahnoun, and V. Togo, Searches for cosmic magnetic monopoles: past, present and future, *Phil. Trans. R. Soc. A* **377**: 20180328 (2019).
- [23] James Pinfold [MoEDAL Collaboration], Technical Design Report of the MoEDAL Experiment, June 8, 2009, 76 pages. Report number: CERN-LHCC-2009-006, MoEDAL-TDR-001
- [24] G. Aad et al. [ATLAS Collaboration], Search for massive long-lived highly ionizing particles with the ATLAS detector at the LHC, *Phys. Lett. B* **698**, 53 (2011).
- [25] G. Aad et al. [ATLAS Collaboration], Search for Magnetic Monopoles in $\sqrt{s} = 7$ TeV pp Collisions with the ATLAS Detector, *Phys. Rev. Lett.* **109**, 261803 (2012),
- [26] G. Aad et al. [ATLAS Collaboration], Search for long-lived, multi-charged particles in pp collisions at $\sqrt{s} = 7$ TeV using the ATLAS detector, *Phys. Lett. B* **722**, 305 (2013).
- [27] S. Chatrchyan et al. [CMS Collaboration], Searches for long-lived charged particles in pp collisions at $\sqrt{s} = 7$ and 8 TeV, *JHEP* **07**, 122 (2013).
- [28] G. Aad et al. [ATLAS Collaboration], Search for heavy long-lived multi-charged particles in pp collisions at $\sqrt{s} = 8$ TeV using the ATLAS detector, *Eur. Phys. J. C* **75**, 362 (2015).
- [29] G. Aad et al. [ATLAS Collaboration], Search for magnetic monopoles and stable particles with high electric charges in 8 TeV pp collisions with the ATLAS detector, *Phys. Rev. D* **93**, 052009 (2016).
- [30] B. Acharya et al. [MoEDAL Collaboration], Search for magnetic monopoles with the MoEDAL prototype trapping detector in 8 TeV proton-proton collisions at the LHC, *JHEP* **08**, 067 (2016).
- [31] B. Acharya et al. [MoEDAL Collaboration], Search for magnetic monopoles with the MoEDAL forward trapping detector in 13 TeV proton-proton collisions at the LHC, *Phys. Rev. Lett.* **118**, 061801 (2017).
- [32] B. Acharya et al. [MoEDAL Collaboration], Search for magnetic monopoles with the MoEDAL forward trapping detector in 2.11 fb⁻¹ of 13 TeV proton-proton collisions at the LHC, *Phys. Lett. B* **782**, 510 (2018).
- [33] B. Acharya et al. [MoEDAL Collaboration], Magnetic Monopole Search with the Full MoEDAL Trapping Detector in 13 TeV pp Collisions Interpreted in Photon-Fusion and Drell-Yan Production, *Phys.Rev.Lett.* **123**, 021802 (2019).
- [34] M. Aaboud et al. [ATLAS Collaboration], Search for heavy long-lived multi-charged particles in proton-proton collisions at $\sqrt{s} = 13$ TeV using the ATLAS detector, *Phys. Rev. D* **99**, 052003 (2018).
- [35] G. Aad et al. [ATLAS Collaboration], Search for Magnetic Monopoles and Stable High-Electric Charged Objects in 13 TeV Proton-Proton Collisions with the ATLAS Detector, *Phys. Rev. Lett.*, **124**, 3 031802 (2020).
- [36] B. Acharya et al. [MoEDAL Collaboration], “First Search for Dyons with the Full MoEDAL Trapping Detector in 13 TeV pp Collisions,” *Phys. Rev. Lett.* **126**, no.7, 071801 (2021).
- [37] B. Acharya et al. [MoEDAL Collaboration], “Search for magnetic monopoles produced via the Schwinger mechanism,” *Nature* **602**, no.7895, 63-67 (2022).
- [38] B. Acharya et al. [MoEDAL Collaboration], Search for highly-ionizing particles in pp collisions at the LHC’s Run-1 using the prototype MoEDAL detector, *Eur.Phys.J. C* **82** (2022) 8, 694; e-Print: 2112.05806 [hep-ex].
- [39] G. Aad et al. [ATLAS Collaboration], Search for heavy long-lived multi-charged particles in the full LHC Run 2 pp collision data at $\sqrt{s} = 13$ TeV using the ATLAS detector, [arXiv:2303.13613 [hep-ex]].
- [40] G. Aad et al. [ATLAS Collaboration], Search for magnetic monopoles and stable particles with high electric charges in $\sqrt{s} = 13$ TeV p-p collisions with the ATLAS detector, arXiv:2308.04835v1 [hep-ex] 9 Aug 2023.
- [41] C. D. Roberts and A. G. Williams, Dyson-Schwinger equations and their application to hadronic physics, *Prog. Part. Nucl. Phys.* **33**, 477-575 (1994).
- [42] D. Binosi and J. Papavassiliou, Pinch Technique: Theory and Applications, *Phys. Rept.* **479**, 1-152 (2009)
- [43] J. Alexandre and N. E. Mavromatos, Weak-U(1) X strong-U(1) effective gauge field theories and electron-monopole scattering, *Phys. Rev. D* **100**, no.9, 096005 (2019). [arXiv:1906.08738 [hep-ph]].
- [44] J. Alexandre, N. E. Mavromatos and V. Mitsou, Resummation Scheme for High-Electric-Charge Objects Leading to Improved Mass Limits, arXiv:2310.17452 [hep-ph], (2023).
- [45] W. Y. Song and W. Taylor, Pair production of magnetic monopoles and stable high-electric-charge objects in proton-proton and heavy-ion collisions, *J. Phys. G* **49**, no.4, 045002 (2022) [arXiv:2107.10789 [hep-ph]].
- [46] J. Ellis, P. Q. Hung and N. E. Mavromatos, *Nucl. Phys. B* **969**, 115468 (2021) [arXiv:2008.00464 [hep-ph]].
- [47] S. Baines, N. E. Mavromatos, V. A. Mitsou, J. L. Pinfold, A. Santra, Monopole production via photon fusion and Drell-Yan processes: MadGraph implementation and perturbativity via velocity-dependent coupling and magnetic moment as novel features, *Eur. Phys. J. C* **78**, 966 (2018).
- [48] V. Andreev et al. [H1 Collaboration], A direct search for stable magnetic monopoles produced in positron-proton collisions at HERA, *Eur. Phys. J. C* **41**, 133 (2005), hep-ex/0501039 [hep-ex].
- [49] B. Abbott et al. [D0 Collaboration], A search for heavy point-like Dirac monopoles, *Phys. Rev. Lett.* **81**, 524 (1998), hep-ex/9803023 [hep-ex].
- [50] J. Alwall, R. Frederix, S. Frixione, V. Hirschi, F. Maltoni,

- O. Mattelaer, H. S. Shao, T. Stelzer, P. Torrielli, and M. Zaro, The automated computation of tree-level and next-to-leading order differential cross sections, and their matching to parton shower simulations, *JHEP* 07, 079, arXiv:1405.0301 [hep-ph].
- [51] R. Ball *et al.* [NNPDF Collaboration], Parton distributions with LHC data, *Nucl. Phys. B* 867, 244 (2013), arXiv:1207.1303 [hep-ph].
- [52] A. Manohar, P. Nason, G. P. Salam, and G. Zanderighi, How bright is the proton? A precise determination of the photon parton distribution function, *Phys. Rev. Lett.* 117, 242002 (2016), arXiv:1607.04266 [hep-ph].
- [53] <https://figshare.com/s/329f3867b27aef555d77>
- [54] E. V Benton and W. D. Nix, The restricted energy loss criterion for registration of charged particles in plastics, *NIM* 67, 343-347 (1969).
- [55] S. Balestra *et al.*, Bulk etch rate measurements and calibrations of plastic nuclear track detectors, *NIM-B* 254, 254-258 (2007).
- [56] K. A. Milton, Theoretical and experimental status of magnetic monopoles, *Rep. Prog. Phys.* 69 (2006) 1637.
- [57] L.P. Gamberg, G.R. Kalbfleisch and K.A. Milton, Direct and indirect searches for low mass magnetic monopoles, *Found. Phys.* 30, 543 (2000) 543; Private communication from Kimball A. Milton, January 26th 2021.
- [58] C.J. Goebel, Binding of nuclei to monopoles, in *Monopole '83*, J.L. Stone ed., Plenum (1984), p. 333.
- [59] L. Bracci and G. Fiorentini, Interactions of Magnetic Monopoles With Nuclei and Atoms, *Nucl. Phys. B* 232, 236 (1984).
- [60] K. Olaussen and R. Sollie, Form-factor effects on nucleus-magnetic monopole binding, *Nucl. Phys. B* 255, 465 (1985).
- [61] A. De Roeck, H. P. Hächler, A. M. Hirt, M. D. Joergensen, A. Katre, P. Mermod, D. Milstead and T. Sloan, *Eur. Phys. J. C* **72**, 2212 (2012).
- [62] A. A. Alves Jr., *et al.* [LHCb Collaboration], The LHCb Detector at the LHC, *JINST* 3, S08005 (2008).